# Supplemental Material

## STED nanoscopy of actin dynamics in synapses deep inside living brain slices

Nicolai T. Urban,[†] Katrin I. Willig,[†] Stefan W. Hell[†] and U. Valentin Nägerl[‡]

[†]Max Planck Institute for Biophysical Chemistry, Göttingen, Germany

[‡]Université de Bordeaux / CNRS, Interdisciplinary Institute for Neuroscience, UMR 5297, F-33000 Bordeaux, France

**Supplemental Movie S1**

**Fast actin dynamics inside dendritic spines**

The movie shows dynamic changes in actin inside dendritic spines. It is a series of 11 maximum intensity projections, based on 10 sections ($\Delta z$ = 500 nm, 30 nm/pixel), and acquired at 1 per minute under baseline conditions.

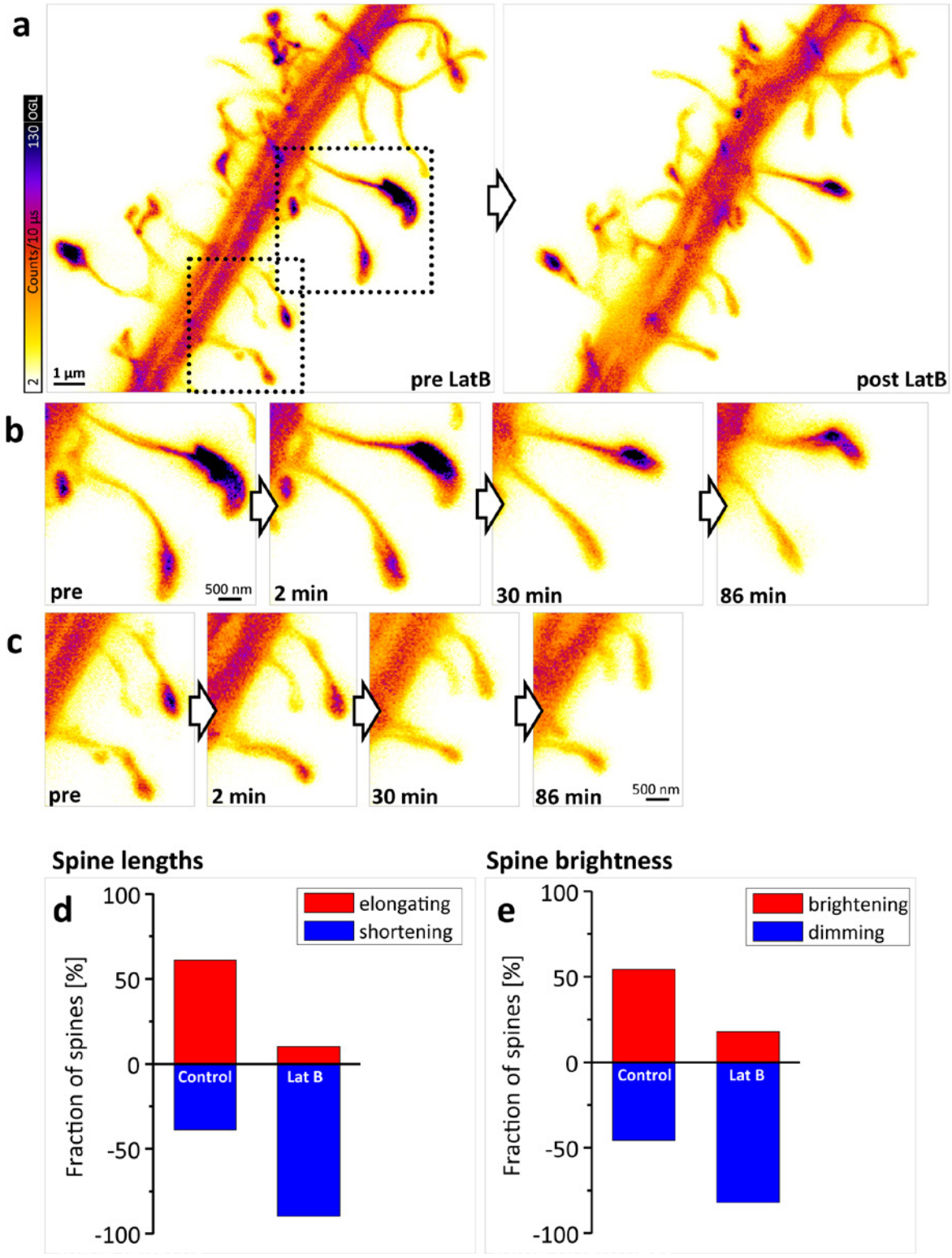


**Supplemental Figure S1**

**Supplemental Figure S1**

**Effects of bath application of Latrunculin B on dendritic spines**

(*a*) STED image of a dendrite belonging to a CA1 pyramidal neuron before (*left panel*) and after (*right panel*) washing in Latrunculin B.

(*b,c*) Zoom-in of the boxed areas in (*a*) exemplifying changes in morphology and actin-concentration in dendritic spines over time.

The first image was recorded before LatB was washed in, all subsequent ones at indicated times after LatB application.

(*d*) Ratio of dendritic spines showing either lengthening or shortening after a comparable amount of time following either perfusion with regular ACSF (control, N=108, *left*) or LatB treatment (N=39, *right*). Spine length was defined as the distance from the base of the spine neck to the tip of the head.

(*e*) Ratio of dendritic spines displaying measurable changes of spine head brightness after a comparable amount of time following either perfusion with regular ACSF (control, N=107, *left*) or LatB treatment (N=39, *right*). Spine head brightness was averaged over a small area around the point of maximum intensity inside the spine head.

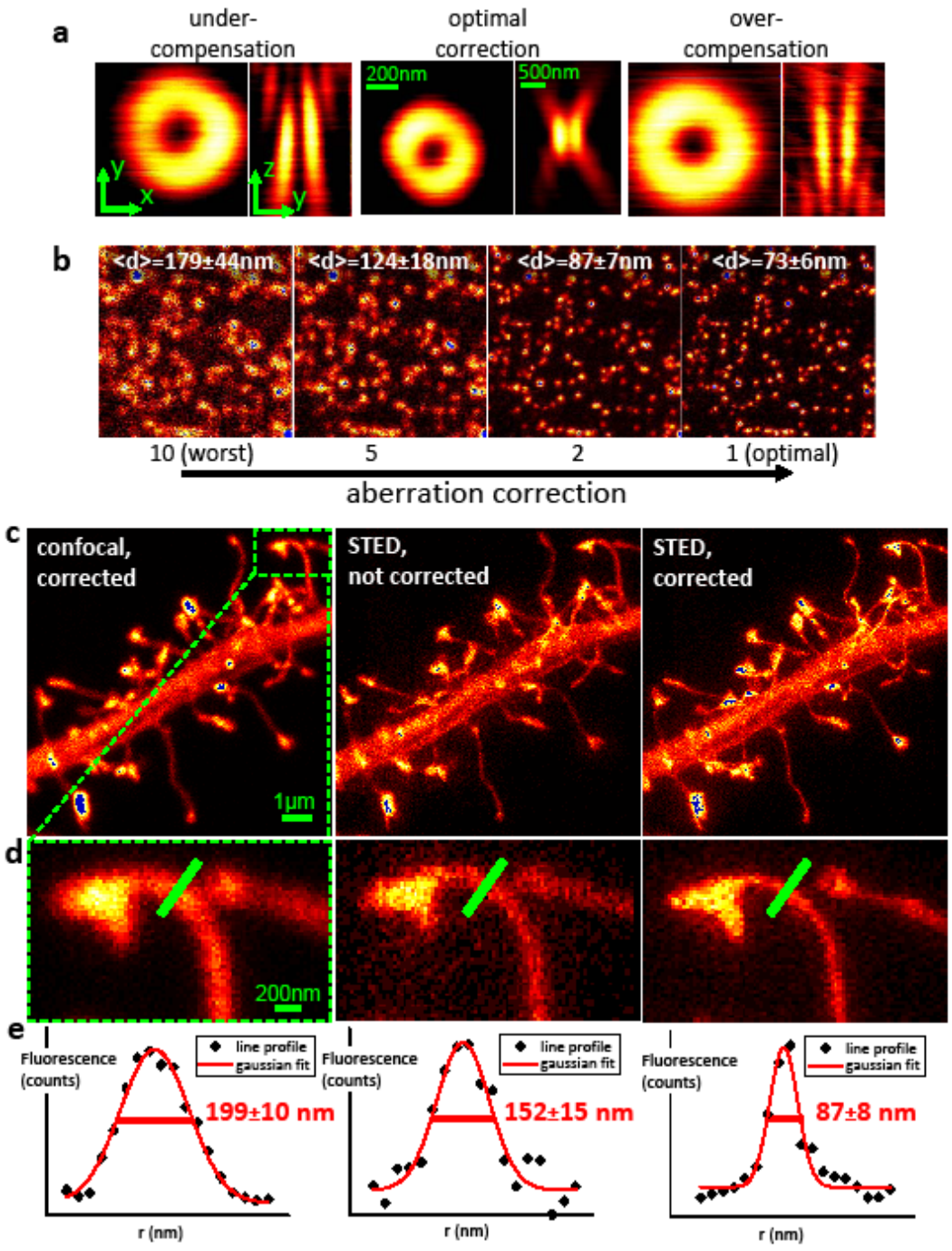


**Supplemental Figure S2**

**Supplemental Figure S2**

**Impact of aberration correction on image quality**

(*a*) STED donut point-spread functions (PSFs) in lateral (x,y) and axial (z) directions for different settings of the correction collar. Under optimal conditions the STED donut is sharply defined in both axial and lateral directions (*center panel*). If the correction collar is misaligned, the PSFs are warped and severely stretched in all directions, especially in axial direction (*left & right panels*).

(*b*) STED images of 40 nm fluorescent yellow-green beads for varying correction collar settings. When the correction collar is misaligned the fluorescent beads are noticeably dimmer and cannot be resolved according to the microscope's full capability (<d> = 179 ± 44nm), even after compensating the loss in brightness with higher excitation powers (*left panel*). If the aberration correction is improved (*from left to right*) the brightness and resolution of the fluorescent beads is noticeably enhanced (2.5-fold, up to <d> = 73 ± 6nm). The indicated values from 1–10 correspond with the correction collar settings, in this case optimal for setting 1 and maximally misaligned for setting 10.

(*c*–*e*) STED images of a dendrite belonging to a CA1 pyramidal neuron for different microscope settings (*c*) and close-ups of two dendritic spines (*d*). In comparison to the confocal image (*left*) the uncorrected STED image is slightly better resolved, but much dimmer (*middle*), whereas the corrected STED image displays substantially enhanced resolution (*right*). Line profiles along the necks of a dendritic spine (*e*) highlight the improved resolution (almost two-fold) after aberration correction.

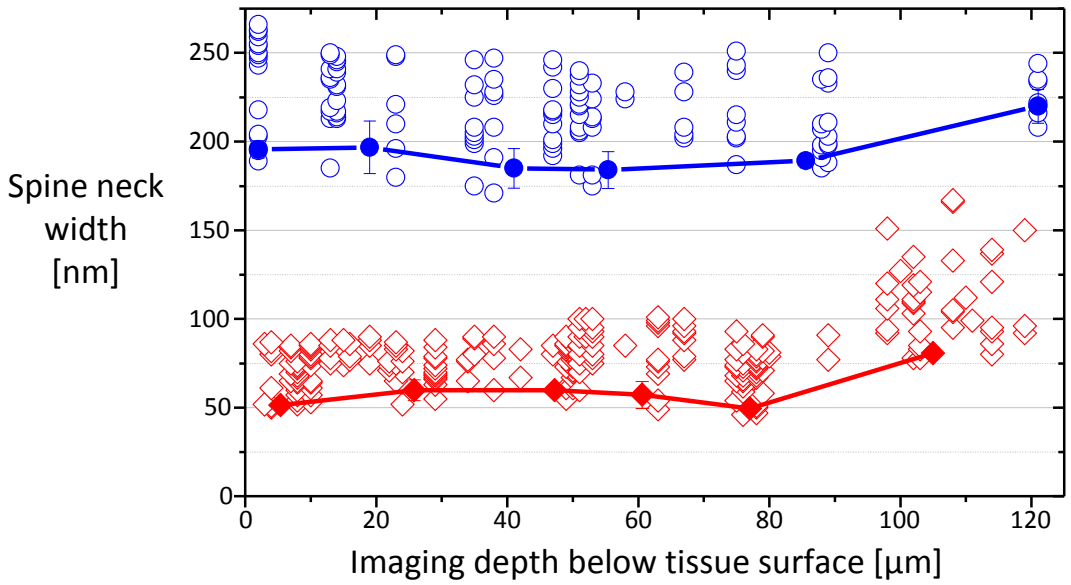


**Supplemental Figure S3**

**Spine neck diameters measured deep inside brain slices**

Spine neck diameters were measured in varying depths inside brain tissue after optimally adjusting the correction collar. Displayed are up to 50 of the thinnest spine necks (FWHMs) per data bin as a function of imaging depth for both confocal (*open circles*) and STED imaging (*open diamonds*). The data bins are 20 µm wide, except for the superficial (0–10 µm) and the deepest layer (90–120 µm). The spatial resolution is estimated for each depth interval by averaging the five smallest FWHM values in that data bin. The estimated resolution for confocal (*solid blue circles*) and for STED microscopy (*solid red diamonds*) remains constant at depths up to 90 µm, after which it starts to deteriorate as the correction collar reached its limit.